

# Accounting for Soil Aging When Assessing Liquefaction Potential

Evangelia Leon<sup>1</sup>; Sarah L. Gassman<sup>2</sup>; and Pradeep Talwani<sup>3</sup>

**Abstract:** It has been recognized that liquefaction resistance of sand increases with age due to processes such as cementation at particle contacts and increasing frictional resistance resulting from particle rearrangement and interlocking. As such, the currently available empirical correlations derived from liquefaction of young Holocene sand deposits, and used to determine liquefaction resistance of sand deposits from in situ soil indices [standard penetration test (SPT), cone penetration test (CPT), shear wave velocity test ( $V_s$ )], are not applicable for old sand deposits. To overcome this limitation, a methodology was developed to account for the effect of aging on the liquefaction resistance of old sand deposits. The methodology is based upon the currently existing empirical boundary curves for Holocene age soils and utilizes correction factors presented in the literature that comprise the effect of aging on the in situ soil indices as well as on the field cyclic strength (CRR). This paper describes how to combine currently recorded SPT, CPT, and  $V_s$  values with corresponding CRR values derived for aged soil deposits to generate new empirical boundary curves for aged soils. The method is illustrated using existing geotechnical data from four sites in the South Carolina Coastal Plain (SCCP) where sand boils associated with prehistoric earthquakes have been found. These sites involve sand deposits that are 200,000 to 450,000 years in age. This work shows that accounting for aging of soils in the SCCP yields less conservative results regarding the current liquefaction potential than when age is not considered. The modified boundary curves indicate that old sand deposits are more resistant to liquefaction than indicated by the existing empirical curves and can be used to evaluate the liquefaction potential at a specific site directly from the current in situ properties of the soil.

**DOI:** 10.1061/(ASCE)1090-0241(2006)132:3(363)

**CE Database subject headings:** Aging; Soils; Liquefaction; Sand; Cementation.

## Introduction

Sand deposits encountered in the South Carolina Coastal Plain (SCCP) are older than 100,000 years. Current empirical correlations that are used to determine liquefaction resistance of sand deposits from in situ soil indices, such as the one proposed by Youd and Idriss (1997), are not valid for the sand deposits in the SCCP because they were derived from relatively young Holocene (<10,000 years) sand deposits. In addition, they are based on historical earthquake events in California, China, and Japan, which have a different style of faulting and site characteristics than the SCCP. Increase in strength and stiffness of sand with time, a phenomenon known as aging, has been reported by many researchers (Mitchell and Solymar 1984; Dowding and Hryciw 1986; Skempton 1986; Schmertmann 1987; Mesri et al. 1990).

Investigation into the different mechanisms that cause aging in sands has not provided explicit evidence so far but is generally focused on chemical and mechanical mechanisms. Chemical mechanisms involve the formation of cementing bonds at particle contacts mainly due to the precipitation of silica from solution (Mitchell and Solymar 1984; Mitchell 1986; Joshi et al. 1995). Mechanical mechanisms involve increasing frictional resistance due to gradual rearrangement of soil particles to a more stable system during secondary consolidation (Schmertmann 1987; Mesri et al. 1990; Arango and Miguez 1996).

Aging has become evident mainly by penetration resistance measurements, where it is reflected in higher blow counts or tip resistance (Mitchell and Solymar 1984; Skempton 1986; Kulhawy and Mayne 1990). Large increases in penetration resistance with time have also been observed following the use of ground modification techniques (Mitchell 1986; Schmertmann 1987; Mesri et al. 1990) such as vibrocompaction and blast densification. Arango and Miguez (1996) and Lewis et al. (1999) have concluded that the field cyclic strength of sand also increases with geologic age, and that this strength increase is not entirely reflected in the sand's penetration resistance. Provided that the most commonly used methods to assess liquefaction potential relate the field cyclic strength (CRR) with in situ soil tests such as the standard penetration test (SPT), the cone penetration test (CPT), and the shear wave velocity test ( $V_s$ ), the liquefaction resistance is likely to be underestimated when using conventional SPT, CPT, or  $V_s$  correlations for sand deposits older than Holocene. There are at present no empirical charts relating SPT blow count, CPT tip resistance, or shear wave velocity  $V_s$  to the field cyclic strength of soil deposits of different geological ages.

<sup>1</sup>Florence & Hutcheson, Inc., Consulting Engineers, 2700 Middleburg Dr., Suite 150, Columbia, SC 29204. E-mail: leon@flohut.com

<sup>2</sup>Associate Professor, Dept. of Civil and Environmental Engineering, Univ. of South Carolina, Columbia, SC 29208. E-mail: gassman@engr.sc.edu

<sup>3</sup>Professor, Dept. of Geological Sciences, Univ. of South Carolina, Columbia, SC 29208. E-mail: talwani@geol.sc.edu

Note. Discussion open until August 1, 2006. Separate discussions must be submitted for individual papers. To extend the closing date by one month, a written request must be filed with the ASCE Managing Editor. The manuscript for this paper was submitted for review and possible publication on January 26, 2004; approved on May 6, 2005. This paper is part of the *Journal of Geotechnical and Geoenvironmental Engineering*, Vol. 132, No. 3, March 1, 2006. ©ASCE, ISSN 1090-0241/2006/3-363-377/\$25.00.

The objective of this study was to develop a methodology to account for the effect of aging on the liquefaction resistance of aged soils. The methodology is based upon the currently existing empirical boundary curves (SPT-, CPT-, and  $V_s$ -based) for Holocene age soils and utilizes correction factors presented in the literature that comprise the effect of aging on the in situ soil indices as well as on the field cyclic strength (CRR). This paper describes how to utilize currently recorded SPT, CPT, and  $V_s$  values and derive corresponding CRR values for aged soil deposits to generate new empirical boundary curves for old sand deposits. The method is illustrated using existing geotechnical data from four sites in the South Carolina Coastal Plain (SCCP) where sand boils associated with prehistoric earthquakes have been found.

## Field Test-Based Evaluation of Liquefaction Potential

One of the most widely accepted and used methods for evaluating soil liquefaction resistance is the Seed et al. (1985) cyclic stress method. The method is a few steps forward of the originally proposed "simplified" method of Seed and Idriss (1971). The approach is based on field observations of the performance of sand deposits that did or did not liquefy in previous earthquakes worldwide. These data have been used to generate simplified curves, which relate surface phenomena such as sand boils, intrusive dikes, or lateral spreading to subsurface liquefaction. The method is based on comparing the earthquake-induced (horizontal) cyclic shear stress to the cyclic resistance of the soil.

The earthquake-induced cyclic shear stress along with the strength and duration of shaking are incorporated in one parameter: the cyclic stress ratio (CSR) which is a function of the earthquake magnitude, peak surface acceleration, the total and effective overburden stress, and the depth of the source bed. The cyclic stress ratio developed in the field due to earthquake shaking can readily be computed

$$CSR = 0.65 \cdot \left( \frac{a_{\max}}{g} \right) \cdot \left( \frac{\sigma_o}{\sigma'_o} \right) \cdot r_d \quad (1)$$

where  $a_{\max}$ =peak horizontal ground surface acceleration;  $g$ =acceleration due to gravity;  $\sigma_o$ =total overburden stress;  $\sigma'_o$ =effective overburden stress; and  $r_d$ =depth-related stress reduction factor decreasing from 1 at the ground surface to 0.9 at a depth of 10 m.

The cyclic resistance of the soil or its resistance to pore pressure buildup is represented by a parameter called cyclic resistance ratio (CRR). The cyclic resistance ratio has been correlated with in situ "index" tests such as the SPT blow count, the CPT tip resistance, and the shear wave velocity of the soil. Accordingly, well-established relationships between CRR and these index tests are available in the literature.

The SPT-based empirical relationship proposed by Seed et al. (1985) with minor modification as recommended by Youd and Idriss (1997) employs  $(N_1)_{60}$  values (SPT blow count  $N$  values corrected for effective overburden stress, energy, and equipment) and is a function of fines content (percentage by weight passing through the U.S. No. 200 sieve). The following equation was recommended to approximate the CRR curve for clean sand (fines content  $\leq 5\%$ ):

$$CRR_{7.5} = \frac{a + cx + ex^2 + gx^3}{1 + bx + dx^2 + fx^3 + hx^4} \quad (2)$$

where  $CRR_{7.5}$ =cyclic resistance ratio for magnitude 7.5 earthquakes;  $x=(N_1)_{60}$ ;  $a=0.048$ ;  $b=-0.1248$ ;  $c=-0.004721$ ;  $d=0.009578$ ;  $e=0.0006136$ ;  $f=-0.0003285$ ;  $g=-1.673E-5$ ; and  $h=3.714E-6$ . This equation is only valid for  $(N_1)_{60}$  less than 30.

For fines content more than 5%, Youd and Idriss (1997) suggested the following fines content correction formula:

$$(N_1)_{60cs} = \alpha + \beta(N_1)_{60} \quad (3)$$

where  $\alpha=0$ ;  $\beta=1.0$  for  $FC \leq 5\%$ ;  $\alpha = \exp[1.76 - (190/FC^2)]$ ;  $\beta = 0.99 + FC^{1.5}/1,000$  for  $5\% < FC < 35\%$ ; and  $\alpha=5.0$ ;  $\beta=1.2$  for  $FC \geq 35\%$  where  $FC$ =fines content in percent.

The CPT-based relationship as recommended by Youd and Idriss (1997) for clean sands and ground motion due to an earthquake of magnitude M7.5 is approximated by the following simplified equation:

$$CRR = 0.833 \left[ \frac{(q_{c1N})_{cs}}{1,000} \right] + 0.05, \quad (q_{c1N})_{cs} < 50 \quad (4)$$

$$CRR = 93 \left[ \frac{(q_{c1N})_{cs}}{1,000} \right]^3 + 0.08, \quad 50 \leq (q_{c1N})_{cs} < 160 \quad (5)$$

The index value employed in this criterion ( $q_{c1N}$ ) is the clean sand cone penetration resistance normalized to 100 kPa.

Another useful index of liquefaction potential, even though the database is quite limited so far, is the shear wave velocity. The  $V_s$ -based empirical relationship proposed by Andrus and Stokoe (2000) is described by the following equation:

$$CRR = a(V_{s1}/100)^2 + b[1/(V_{s1}^* - V_{s1}) - 1/V_{s1}^*] \quad (6)$$

where  $a=0.022$  and  $b=2.8$  are the curve fitting parameters;  $V_{s1}$ =corrected (to 100 KPa) shear wave velocity accounting for overburden pressure;  $V_{s1}^*$ =limiting upper value of  $V_{s1}$  for cyclic liquefaction occurrence and can be expressed by

$$V_{s1}^* = 215 \text{ m/s}, \quad \text{for sands with } FC \leq 5\% \quad (7)$$

$$V_{s1}^* = 215 - 0.5(FC - 5) \text{ m/s}, \quad \text{for sands with } 5\% < FC < 35\% \quad (8)$$

$$V_{s1}^* = 200 \text{ m/s}, \quad \text{for sands and silts with } FC \geq 35\% \quad (9)$$

Each empirical curve relates a resistance parameter of the individual test [ $(N_1)_{60}$ ,  $q_{c1}$ ,  $V_{s1}$ ] to the soil's resistance to cyclic loading (CRR). Points along the CRR curve are considered as the capacity of the soil to resist the cyclic shear stresses induced by an earthquake M7.5 for a given  $(N_1)_{60}$ ,  $q_{c1}$ , or  $V_{s1}$  measurement. All curves divide sites that liquefied ( $CSR > CRR$ ) from those that did not ( $CSR < CRR$ ) on the basis of  $(N_1)_{60}$ ,  $q_{c1}$ , and  $V_{s1}$ .

The SPT, CPT, and  $V_s$  can be easily and economically obtained today leading to a routine use of these empirical relationships in the assessment of the liquefaction potential of sand deposits. However, these correlations pertain to Holocene-age (<10,000 years) soil deposits, derived predominantly from postearthquake field investigations, and are not strictly valid for evaluating the CRR for older than Holocene soils.

## Soil Aging Effects

### *Historical Background*

Youd and Hoose (1977) and Youd and Perkins (1978) were among the first to note that liquefaction resistance of sands increases markedly with geologic age. Based on their observations, sediments deposited within the past few hundred years are generally more susceptible to liquefaction than older Holocene (<10,000 years) sediments. Pleistocene sediments are even more resistant, and Pre-Pleistocene sediments are essentially liquefaction resistant. The potential mechanism reported by Youd and Hoose (1977) to explain the reduction in liquefaction susceptibility with age was the cementing and compaction of the soil by natural processes, as well as changes in topography, water table depth, and depth of burial due to postdepositional geologic processes. Youd and Perkins (1978) developed a procedure using geologic and seismologic information in compiling maps showing liquefaction-induced ground failure potential based on geologic and seismologic information. Age of depositions was included among the different factors (sedimentation process, geologic history, depth of water table, grain size distribution, density state, depth of burial, ground slope, nearness of a free face) that affect ground failure susceptibility.

Mitchell and Solymar (1984) and Mitchell (1986) detected the increase in stiffness and strength that freshly deposited sands are likely to develop, as measured by resistance to penetration over periods up to several months. Mitchell and Solymar (1984) compared laboratory and field data to illustrate the time dependent increases in stiffness, penetration resistance, resistance to cyclic mobility, and strength gain in clean sands following deposition, placement, or densification. They concluded that the stiffness and strength, as measured by resistance to penetration, increase over periods up to several months, and can be as much as twice the initial penetration resistance value. Mitchell (1986) illustrated some of the problems that led to the conclusion that soils are not inert materials, but they change with time. One of the problems that he refers to is the time effects in freshly densified or deposited sand, in which natural sand deposits can lose strength if disturbed but regain strength over time periods of weeks or months. CPT records before and after a blasting densification test suggested that a reduction in penetration resistance was caused shortly after the in situ densification, but substantial increases in penetration resistance had developed over a period of several months.

Mitchell and Solymar (1984) and Mitchell (1986) suggested that aging is a result of chemical mechanisms such as the formation of silica acid gel on particle surfaces and silica precipitates from solution. These precipitates cause cementing bonds at interparticle contacts. Evidence supporting this mechanism was presented by Joshi et al. (1995) who studied the effect of aging on the penetration resistance of freshly deposited sands, based on tests conducted on two sands in a submerged and dry state. The samples were allowed to age for 2 years in the laboratory. The micrographs of the freshly deposited sands and the sands with dry aging showed no evidence of precipitates. However, the presence of precipitates connecting the sand grains of the samples with submerged aging was obvious in the micrographs. For the case of the dry sands mechanical mechanisms such as macrointerlocking of particles and microinterlocking of surface roughness due to an externally applied load were suggested by Joshi et al. (1995). This is similar to the mechanism proposed earlier by Schmertmann (1987) in a discussion of the paper by Mitchell and Solymar

(1984). Schmertmann (1987) presented data on the time-dependent increase in cone resistance of clean sands after dynamic dropped-weight compaction. He considered the processes that take place during secondary compression and found that during secondary consolidation gradual rearrangement of soil particles to a more stable system results in an increase of the number of interparticle contacts improving the grain surface roughness.

Mesri et al. (1990) observed an increase in stiffness of sand due to aging under consolidated or densified conditions. Examples of the aging on the small strain shear modulus and cone penetration resistance from the literature were presented, and the writers attributed this increase in strength to the improved frictional resistance that develops during secondary compression. During secondary compression (drained aging) resistance increases due to a decrease in density resulting from the continuous rearrangement of the sand particles. This mechanism causes an increased macrointerlocking of sand grains and microinterlocking of grain surface roughness.

One year later, Schmertmann (1991), in his Terzaghi lecture, presented many examples of aging improvement in sand (and other soils) behavior, including laboratory and field experience. He indicated that aging effects are the result of increased in situ effective stresses including grain slippage, dispersive particle movements, increased grain interlocking, and internal stress arching. Olson et al. (2001) considers that in the short term of hundreds to a few thousands of years, mechanical effects caused by adjustment of grains during secondary consolidation are likely to dominate aging. However, over geologic time chemical cementation may become significant.

### *Aging of Sands in the SCCP*

Geologic processes that have taken place in the SCCP over time indicate several factors that may have contributed to the aging effect in the old sand deposits. These include mechanical and chemical action associated with the beach environment of the SCCP. Geologic evidence from wells and surface exposures indicates that sea level has fluctuated through many cycles during geologic time. During cyclic wet and dry periods soluble materials are carried in solution when the sea level increases and precipitate when the sea level is lowered leading to the formation of cementation bonds between the soil particles. When the sea level rises soluble materials are carried in solution and precipitated again as a result of changed conditions (lowering of sea level). In addition the action of water causes rounding and polishing of the sand grains leading to changes in packing and interparticle friction.

Two previous studies evaluated the dynamic strengths of geologically old sand deposits from the SCCP and suggested higher resistance to liquefaction than that indicated by the existing empirical charts for young Holocene age soils. The first study was carried out by Bechtel Savannah River, Inc. (BSRI 1993, 1995). Two Miocene-age (30 million years old) sand deposits from the Tobacco Road and Dry Branch formations in west South Carolina were tested under undrained stress-controlled cyclic triaxial loading. The tests were performed on undisturbed thin wall tube soil samples obtained from two investigated sites in the location of the Savannah River Site (SRS) [referred to as ITP and RTF in BSRI (1995)]. In situ tests such as SPT and CPT were performed at these sites as well. The findings were also compared with the strength of clean Holocene sands (Seed et al. 1983) as shown in

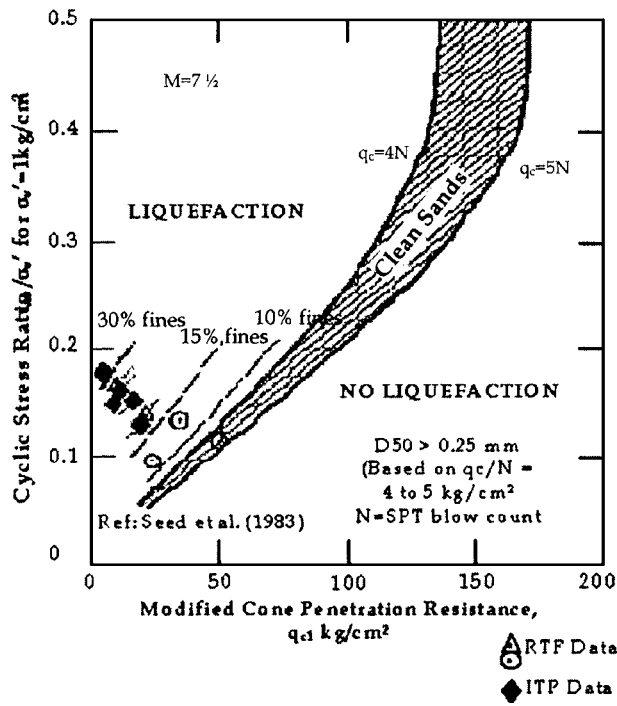


Fig. 1. Proposed correlation for ITP and RTF sites between modified cone tip resistance and cyclic stress ratio [adapted from BSRI (1995)]

Fig. 1. Site specific results demonstrate a higher resistance to liquefaction than would be predicted by the existing empirical chart.

The second study by Lewis et al. (1999) incorporated studies by different researchers who performed geotechnical investigations at discovered paleoliquefaction sites in and around Charleston, S.C. in soil deposits ranging in age from recent to older than 200,000 years. For their evaluation the expected meizoseismal acceleration of 0.3g–0.5g and data from sites ranging in age from 85,000 to 200,000 years old were used. Given the simplified approach proposed by Seed and Idriss (1971) the cyclic stress ratios were determined for each site and plotted with the appropriate  $(N_1)_{60}$  values in the same chart with the Seed et al. (1984) empirical correlation valid for Holocene age soils only. Fig. 2 presents the results for 0.5g meizoseismal acceleration induced by the 1886 Charleston earthquake and resulted in liquefaction, marginal liquefaction, or no liquefaction. The lower (dashed line) and upper (continuous line) curves show the minimum and maximum, respectively, stress ratio values required to cause liquefaction for those sites that experienced marginal liquefaction and liquefaction. These were compared with the existing boundary curves for Holocene age sands (Seed et al. 1984). For meizoseismal accelerations 0.5g and 0.3g the results suggest strengths 2 to 3 times and 1.3 to 1.8 times higher, respectively, than those predicted by the existing empirical chart. The differences observed were attributed to aging effects of the sand deposits encountered at the specific sites.

### Impact of Soil Aging on Testing Procedures

Even though the mechanisms that cause aging in sand are not well understood, it is important to show that they are reflected in the results of different tests. There is evidence that soil aging in-

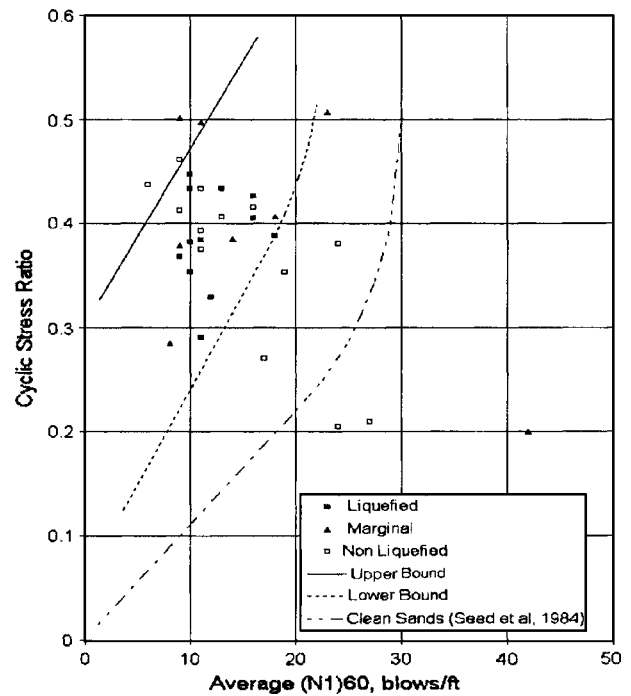


Fig. 2. Normalized penetration resistance versus cyclic stress ratio induced by the 1886 Charleston earthquake that resulted in liquefaction, marginal liquefaction, or no liquefaction [Lewis et al. (1999), with permission]

creases the in situ soil indices (SPT blow count, CPT tip resistance, and shear wave velocity), as well as the field cyclic strength of the soil as expressed by CRR.

Skempton (1986) studied the increase in the SPT blow count with time in five sand soil deposits and concluded that the aging effect is reflected in higher blow count and the resistance of sand to deformation is greater the longer the period of consolidation. Kulhawy and Mayne (1990) collected field and laboratory data on SPT blow count and relative density of both normally consolidated and overconsolidated unaged fine to medium fine sands. The corrected blow count  $(N_1)_{60}$  was used to evaluate the relative density  $D_r$  as a function of the soil particle size ( $D_{50}$ ). The following empirical relationship was suggested to determine the relative density of the soil based on the measured penetration resistance for normally consolidated unaged sands. It is assumed that the relative density of the sand deposit remains constant during the entire period:

$$\frac{(N_1)_{60}}{D_r^2} = 60 + 25 \log D_{50} \quad (10)$$

Overconsolidated sands and aged sands give higher values than those determined by Eq. (10). Another set of data representing aged fine to medium sands, likely overconsolidated, of four geologic periods was plotted as a function of the age of the deposit by Kulhawy and Mayne (1990) (Fig. 3). A correction factor  $c_A$  was introduced to describe the influence of aging ( $t$ , in years) on the  $(N_1)_{60}/D_r^2$  ratio and according to F. H. Kulhawy (personal communication, 2003) the same coefficient can be applied to CPT tip resistance data

$$c_A = 1.2 + 0.05 \log(t/100) \quad (11)$$

Based on the assumption that cone penetration resistance is mainly determined by stiffness of sand and effective horizontal

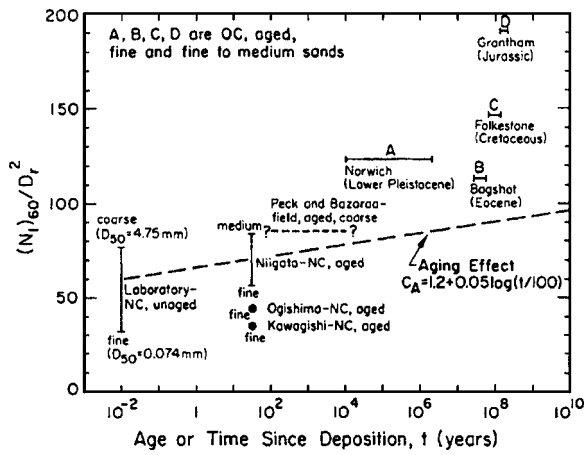


**Fig. 3.** Aging effect on blow counts for sands [from Kulhawy and Mayne (1990), copyright© 1990, Electric Power Research Institute, E L-1990, *Manual on Estimating Soil Properties for Foundation Design*, reprinted with permission]

stress, Mesri et al. (1990) proposed an empirical equation that can be used to estimate the increase in cone penetration resistance of clean sands with time:

$$\frac{q_c}{(q_c)_R} = \left(\frac{t}{t_R}\right)^{C_D C_a / C_c} \quad (12)$$

where  $(q_c)_R$  and  $t_R$  = values of cone penetration resistance and time at the end of primary consolidation or some other reference time and  $q_c$  = cone resistance at any time  $t > t_R$ .  $t_R$  corresponds to the number of days after which the postdensification  $q_c$  value was measured by Mesri et al. (1990) and ranged from 1 to 30 days.  $C_a / C_c$  = the ratio of secondary compression index to compression index which was found to range between 0.015 and 0.03 for at least nine different sands in the laboratory over a stress range of 50–3,000 KPa. The writers suggest that for practical purposes  $C_a / C_c$  for sands can be considered constant and equal to 0.02.  $C_D$  = empirical parameter introduced to account for the effect of densification due to ground improvement.

Blast densification data of Dowding and Hryciw (1986) and deep densification data of Mitchell and Solymar (1984) were used to calibrate Eq. (12) by adjusting the parameter,  $C_D$ , until predicted values matched well with the field data. The resulting values of  $C_D$  with respect to the change in relative density,  $\Delta e_R$ , resulting from postliquefaction densification, a process similar to consolidation, are shown in Fig. 4. The value of  $\Delta e_R$  was estimated by Ellis and De Alba (1999) to be around 4 to 5%. Stark et al. (2002) suggest the value of the same parameter to be around 4–10%. According to Olson et al. (2001), since both CPT and SPT penetration resistances are affected similarly by soil compressibility and horizontal effective stress, a similar equation can be derived to account for the increase in SPT following densification, by substituting  $N_{60}$  for  $q_c$  in Eq. (12). For values of the penetration resistance compared at the same depth,  $N_{60}$  is substituted by  $(N_1)_{60}$  and  $q_c$  is substituted by  $q_{c1}$

$$\frac{q_{c1}}{(q_{c1})_R} = \frac{(N_1)_{60}}{[(N_1)_{60}]_R} = \left(\frac{t}{t_R}\right)^{C_D C_a / C_c} \quad (13)$$

where  $[(N_1)_{60}]_R$  and  $(N_1)_{60}$  = SPT blow count at some reference time  $t_R$  and at any time  $t > t_R$ , respectively.

Joshi et al. (1995) studied the effect of aging on the penetration resistance of freshly deposited sands, based on tests con-

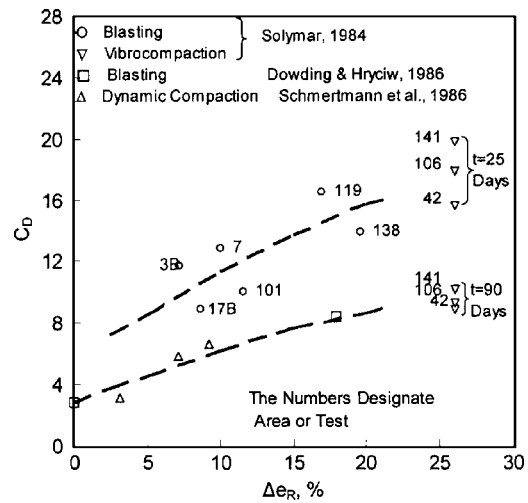


**Fig. 4.** Summary of  $C_D$  data for ground-modification projects [Mesri et al., (1990), ASCE]

ducted on two sands in a submerged and dry state. The aging phenomena were approximated by an exponential equation, similar to the equation given by Mesri et al. (1990) for postdensification of sand

$$\frac{P_t}{P_1} = a(t)^b \quad (14)$$

where  $t$  = aging period expressed in days;  $P_t$  = penetration resistance at age  $t$ ;  $P_1$  = penetration resistance of freshly deposited sand on the first day; and  $a$  and  $b$  = constants depending on the environmental conditions of the sand. However, this equation is dependent upon the externally applied load. The higher the consolidation load, the faster the aging.

Arango et al. (2000) demonstrated that age plays a major role in the field cyclic strength of sand deposits based on data from four separate site-specific investigations. The correlation that they proposed for the strength gain factor was based on an update of the correlation that was proposed earlier by Kramer and Arango (1998) and is represented in Fig. 5 by the heavy line. It was drawn

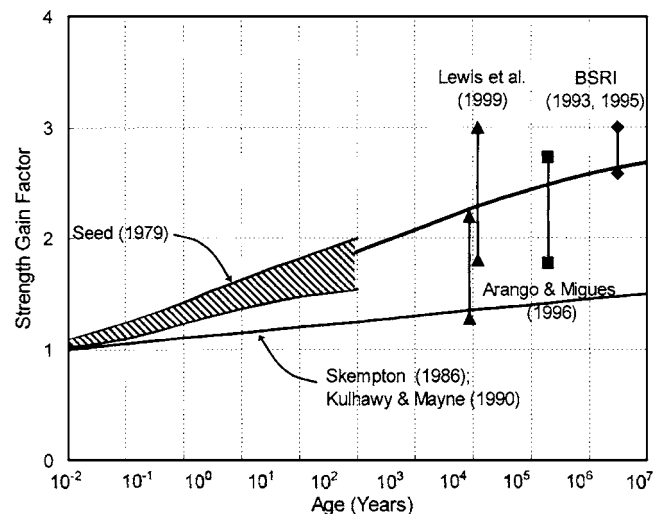


**Fig. 5.** Field cyclic strength of aged sand deposits: Updated relationship [adapted from Arango et al. (2000)]

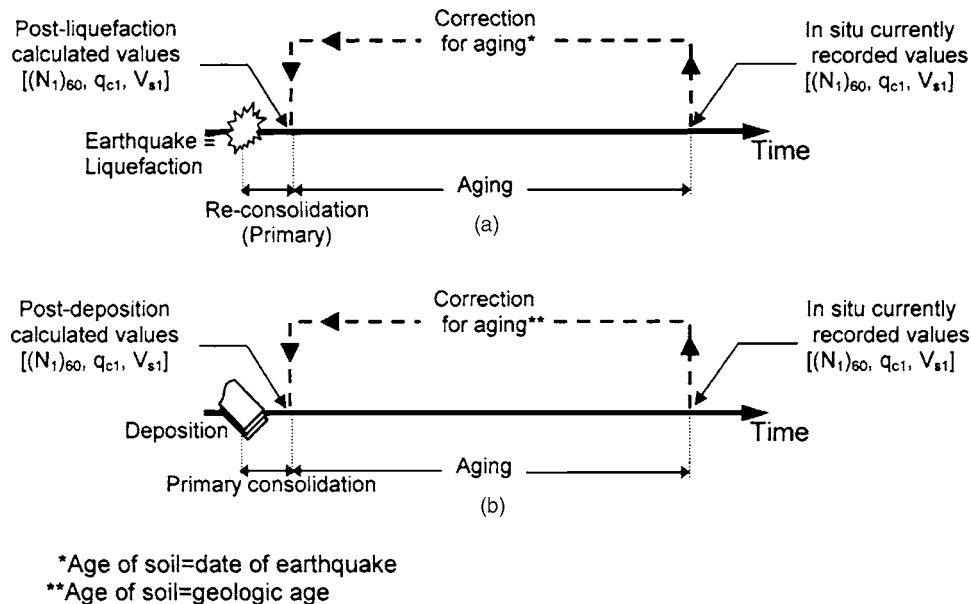


**Fig. 6.** Correction of in situ currently recorded values of  $(N_1)_{60}$ ,  $q_{c1}$ , or  $V_{s1}$  for the effect of aging for (a) liquefied sites, and (b) nonliquefied sites

in such a way as to be compatible with the results of previous studies by Seed (1979); BSRI (1993); Arango and Migues (1996); BSRI (1995); and Lewis et al. (1999). The first study carried out by Seed (1979) reported results from laboratory experiments conducted on identical samples that were subjected to sustained loads for a period ranging from 0.1 to 100 days. The samples subjected to longer periods of sustained loading showed an increased resistance to initial liquefaction of about 25%. Seed also compared the cyclic strength resistance of undisturbed samples obtained from an old fill with those of freshly deposited samples of the same sand. He reported strength increases on the order of 50–100% in 1,000 years over those of the recent deposits. In the study by Arango and Migues (1996), reconstituted and undisturbed block specimens from the Tapo Canyon formation (1 to 2 million years old) were cyclically tested in the laboratory under stress-controlled undrained conditions. A technique of controlled freezing and thawing of saturated, undisturbed specimens was performed in an effort to impose small but uniform strains to the specimen volumetrically, but without the complete destruction of fabric that accompanies remolding. Based on the strength range that was estimated, the field aged cyclic strength of the Tapo Canyon sand (a relatively uniform, fine sand with sand grains consisting of predominately quartz and a lesser amount of feldspar particles) was 1.6–2.7 times greater than estimated by conventional empirical charts. In the study carried out by Bechtel Savannah River, Inc. (BSRI 1993, 1995) 30 million-years-old sand deposits from the Tobacco Road and Dry Branch formation in west South Carolina were found to have 2.6–3 times higher cyclic strengths than the one predicted by the existing empirical chart. Finally from the Charleston-site-specific boundary curves presented by Lewis et al. (1999) it was suggested that cyclic strengths are 1.3–3 times higher than those predicted by the empirical chart for Holocene age soils.

The correlations proposed by Skempton (1986); and Kulhawy and Mayne (1990) are demonstrated in Fig. 5 along with the one proposed by Arango et al. (2000). The increase with time as represented by the “strength gain factor” is illustrated by both curves, although for different types of data. The correlation proposed by Skempton (1986) and Kulhawy and Mayne (1990) demonstrates

an increase in SPT blow count, whereas the latter correlation proposed by Arango et al. (2000) and represented by the heavy line demonstrates an increase in the field cyclic strength (CRR) of the sand deposit with increasing age. Although there is an agreement in the general trend of the two curves, the penetration resistance-based curve predicts lower strength gains.

Thus the factors that cause aging in the sand are apparent in the increasing penetration resistance (and probably shear wave velocity) with age to a lesser degree than they are in the increasing liquefaction resistance (as expressed by CRR). According to Arango and Migues (1996) penetration resistance is a poor indicator of the in situ conditions of the sand deposit when aging is encountered. Since penetration resistance does not fully capture the effect of aging of the soil the existing penetration resistance-based curves may conservatively estimate the liquefaction resistance for old soil deposits. The inability of the SPT and CPT tests to capture the effect of aging is attributed to the nature of these tests which are not sufficiently sensitive to detect minor changes in soil fabric that can increase the liquefaction resistance of the soil. The effect of disturbance during the tests can be significant thereby destroying the macrostructure of the soil and consequently the aging factors that are present. Likewise, but to a much smaller degree, the small-strain shear wave velocity measurements are anticipated to disturb the existent aging factor.

### Proposed Methodology

The empirical correlations for liquefaction evaluation applicable for young or “freshly deposited” soils can be used for older soil deposits as long as the parameters involved (SPT, CPT,  $V_s$ , and CRR) are modified appropriately to account for the effect of aging. To assess the liquefaction potential of the aged soil deposits using the existing empirical correlations, the postearthquake penetration resistance or shear wave velocity of the soil should be employed. In this work the “postearthquake” and “freshly deposited” terms are used interchangeably. A schematic explanation is demonstrated in Fig. 6 for two different scenarios: sites with evi-

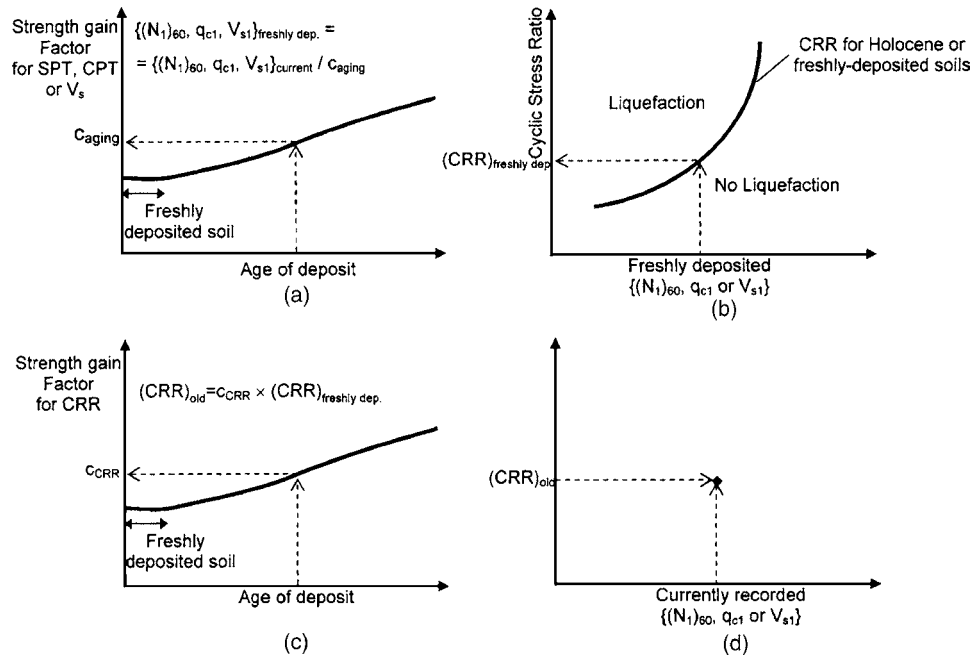


**Fig. 7.** Proposed methodology: (a) Step 1—correction of in situ currently recorded data for aging, (b) Step 2—determination of CRR for freshly deposited soil, (c) Step 3—determination of CRR for old/aged soil deposit, and (d) Step 4—association of in situ currently recorded data with CRR for old/aged soil deposit

dence of liquefaction and sites with no evidence of liquefaction. For sites that liquefied and are thus associated with a prehistoric earthquake [Fig. 6(a)] the freshly deposited condition coincides with the postliquefaction condition. In this case aging covers the period of time from the date the field tests were performed to the date of occurrence of the associated earthquake that caused liquefaction. It is assumed that no more liquefaction events have disrupted the soil structure during this period of time. For sites that did not liquefy [Fig. 6(b)] the freshly deposited condition describes the condition after the deposition of the soil. In this case aging covers as much time as the geologic age of the deposit assuming that no liquefaction event has ever disrupted the soil structure.

Provided that aging effects reestablish themselves with time after the occurrence of liquefaction (or deposition), their effect on the SPT, CPT,  $V_s$ , and CRR is taken into account with a four-step recommended procedure as shown in Fig. 7. As a first step [Fig. 7(a)], the in situ currently recorded values of  $\{(N_1)_{60}, q_{c1},$  or  $V_{s1}\}$  are corrected for the effect of aging using the Kulhawy and Mayne (1990) and/or the Mesri et al. (1990) method. The Kulhawy and Mayne (1990) method specifies that the  $(N_1)_{60}$  and  $q_{c1}$  values are corrected by the correction factor  $c_A$  described by Eq. (11). The Mesri et al. (1990) method specifies a different correction factor for the  $(N_1)_{60}$  and  $q_{c1}$  values given by the right-hand side of Eq. (13). For both methods the correction factor that is applied on the  $V_{s1}$  values is derived by converting the  $V_{s1}$  to equivalent  $q_{c1}$  values where the correction factor  $c_A$  [for the Kulhawy and Mayne (1990) method] or  $(t/t_R)^{C_D C_d' C_C}$  [for the Mesri et al. (1990) method] can be applied. To this end the following correlation proposed by Andrus et al. (2003) is employed:

$$V_{s1} = 77.4(q_{c1N})^{0.178} ASF \quad (15)$$

where shear wave velocity ( $V_s$ );  $q_{c1N}$ =normalized, stress-corrected cone penetration resistance ( $q_{c1}$ ); and  $ASF$  is an aging scaling factor which is equal to 1.00 for Holocene age deposits

(<10,000 years) and equal to 1.41 for Pleistocene age deposits (10,000 <  $t$  < 1.5 million years).

Thus the increase in  $(N_1)_{60}$ ,  $q_{c1}$ , and  $V_{s1}$  with age for the Kulhawy and Mayne (1990) method can be described by the following equation:

$$\frac{(N_1)_{60}}{[(N_1)_{60}]_R} = \frac{q_{c1}}{(q_{c1})_R} = \left[ \frac{(V_{s1})}{(V_{s1})_R} \right]^{1/0.178} = c_A \quad (16)$$

and for the Mesri et al. (1990) method

$$\frac{(N_1)_{60}}{[(N_1)_{60}]_R} = \frac{q_{c1}}{(q_{c1})_R} = \left[ \frac{(V_{s1})}{(V_{s1})_R} \right]^{1/0.178} = \left( \frac{t}{t_R} \right)^{C_D C_d' C_C} \quad (17)$$

where  $[(N_1)_{60}]_R$ ,  $(q_{c1})_R$ , and  $(V_{s1})_R$ =SPT, CPT, and shear wave velocity values, respectively, at a reference time  $t_R=0$  which chronologically coincides with the freshly deposited state of the soil (after liquefaction or deposition); and  $(N_1)_{60}$ ,  $q_{c1}$ , and  $V_{s1}$ =SPT, CPT, and shear wave velocity values, respectively, at any time  $t > 0$  or the currently recorded values. By incorporating correction factors  $c_A$  and  $(t/t_R)^{C_D C_d' C_C}$  into a parameter  $c_{\text{aging}}$  the following general equation describes the evaluation of the  $(N_1)_{60}$ ,  $q_{c1}$ , and  $V_{s1}$  values of the soil at its freshly deposited state for both the Kulhawy and Mayne (1990) and Mesri et al. (1990) methods

$$\{(N_1)_{60}, q_{c1}, V_{s1}^{1/0.178}\}_{\text{freshly dep.}} = \frac{\{(N_1)_{60}, q_{c1}, V_{s1}^{1/0.178}\}_{\text{current}}}{c_{\text{aging}}} \quad (18)$$

Once the postearthquake penetration resistance and shear wave velocity of the soil have been estimated, the corresponding CRR of the freshly deposited soil (immediately after liquefaction for liquefied or deposition for nonliquefied sites) can be evaluated from the existing empirical correlations as a second step [Fig. 7(b)]. Eqs. (2) and (3) are employed for the SPT-based evaluation, Eqs. (4) and (5) for the CPT-based evaluation, and Eqs. (6)–(9) for the  $V_s$ -based evaluation.

**Table 1.** In Situ Geotechnical Data for Source Sands [Data Adapted from Hu et al. (2002a)]

| Site            | Location | $z$<br>(m) | $h$<br>(m) | $\sigma_o$<br>(kPa) | $\sigma'_o$<br>(kPa) | $(N_1)_{60}$    | $q_{c1}$<br>(MPa) | $V_{s1}$<br>(m/s) | Fines<br>(%) | $D_{50}$<br>(mm) |
|-----------------|----------|------------|------------|---------------------|----------------------|-----------------|-------------------|-------------------|--------------|------------------|
| Gapway          | GAP-01   | 2          | 0.7        | 36                  | 36                   | 10              | 3.1               | 181               | N/A          | —                |
|                 | GAP-02   | 2          | 0.9        | 36                  | 36                   | 11 <sup>a</sup> | 5.5               | 220               | 9            | 0.15             |
|                 | GAP-03   | 2          | 1.0        | 36                  | 36                   | 11              | 8.3               | 177               | 6            | 0.19             |
|                 | GAP-04   | 2          | 1.1        | 36                  | 36                   | 8               | 7.9               | 240               | N/A          | —                |
|                 | GAP-05   | 2          | 1.3        | 36                  | 36                   | 16              | 8.6               | 154               | 5            | 0.20             |
| Sampit          | SAM-01   | 4          | 5.7        | 71                  | 55                   | 14 <sup>a</sup> | 10.9              | 277               | 3            | 0.17             |
|                 | SAM-02   | 6          | 4.3        | 108                 | 73                   | 14 <sup>a</sup> | 10.4              | 250               | 1            | 0.16             |
|                 | SAM-03   | 5          | 5.2        | 89                  | 64                   | 14 <sup>a</sup> | 7.4               | 288               | 0            | 0.20             |
|                 | SAM-04   | 5          | 5.4        | 89                  | 61                   | 14              | 7.7               | 291               | 2            | 0.18             |
|                 | SAM-05   | 5          | 5.8        | 89                  | 57                   | 16              | 9.0               | 334               | 4            | 0.20             |
|                 | SAM-06   | 5          | 5.6        | 89                  | 61                   | 9               | 7.7               | 321               | 4            | 0.16             |
| Ten Mile Hill A | TEN-01   | 2          | 1.5        | 36                  | 33                   | 18              | 15.6              | 235               | 7            | 0.16             |
|                 | TEN-02   | 3          | 1.5        | 54                  | 40                   | 30              | 19.5              | 400               | 3            | 0.16             |
|                 | TEN-03   | 3          | 2.4        | 54                  | 40                   | 17              | 15.3              | 163               | 3            | 0.16             |
|                 | TEN-04   | 3          | 2.7        | 54                  | 40                   | 18              | 8.0               | 214               | 3            | 0.16             |
|                 | TEN-05   | 4          | 2.4        | 71                  | 56                   | —               | 14.6              | 239               | —            | —                |
| Ten Mile Hill B | TEN-06   | 4          | 3.8        | 71                  | 56                   | 9               | 4.4               | 170               | 4            | 0.17             |
|                 | TEN-07   | 5          | 4.1        | 89                  | 65                   | 5               | 5.4               | 187               | 5            | 0.17             |
|                 | TEN-08   | 5          | 4.2        | 89                  | 65                   | 8               | 5.5               | 177               | 4            | 0.16             |
|                 | TEN-09   | 5          | 4.3        | 89                  | 73                   | 5               | 5.8               | 158               | 5            | 0.17             |
|                 | TEN-10   | 6          | 5.3        | 108                 | 81                   | 6               | 6.3               | 165               | 5            | 0.17             |

Note:  $z$ =depth of the middle point of source sand layer;  $h$ =thickness of source sand layer;  $\sigma_o$ ,  $\sigma'_o$ =total overburden stress and effective overburden stress at the middle point of source sand layer;  $(N_1)_{60}$ =corrected SPT blow count number;  $q_{c1}$ =corrected CPT tip resistance;  $V_{s1}$ =normalized shear-wave velocity; Fines: percentage by weight passing through U.S. No. 200 sieve;  $D_{50}$ =grain diameter corresponding to 50% passing (by weight) the No. 200 sieve.

<sup>a</sup>The blow count values at SAM-01 to SAM-03 are based on data from SAM-04 and at GAP-02 to GAP-05 on the data from GAP-03.

The third step is to evaluate the current CRR value for the aged soil deposit considering that over the hundreds or thousands of years that follow the earthquake (for liquefied sites) or deposition of the soil (nonliquefied sites), as aging effects reestablish themselves, resistance to liquefaction generally continues to increase [Fig. 7(c)]. To this end the correlation for the strength gain factor proposed by Arango et al. (2000) is employed. In this case by “strength” the CRR of the soil is implied and the strength gain factor,  $c_{CRR}$ , is defined as the ratio of the strength of the soil after a period under “aging” over the strength of the soil at its freshly deposited state:

$$c_{CRR} = \frac{(CRR)_{aged/current}}{(CRR)_{freshly\ dep.}} \quad (19)$$

where  $c_{CRR}$  is obtained by the heavy line in Fig. 5 for the specific age of the soil. Similarly to the first step, the age of the soil is equal to the date of the earthquake for liquefied sites associated with a specific prehistoric earthquake and equal to the geologic age of the deposit for nonliquefied sites.

Finally, the currently recorded penetration resistance or shear wave velocity values are plotted with  $(CRR)_{aged/current}$  values determined in the third step for each one of the locations where liquefaction evidence was or was not found [Fig. 7(d)]. Using all the locations the best-fit curve is plotted which constitutes the liquefaction resistance curve for old sand deposits.

## Data

The proposed methodology is illustrated using geotechnical data from four paleoliquefaction sites in the SCCP that were first examined by Hu et al. (2002a). These data included SPT, CPT, and shear wave velocity data from tests performed at locations of known sand boils and locations where no sand boils were observed. The four paleoliquefaction sites were Ten Mile Hill sites A and B with sand deposits of 200,000 years in age, and Sampit

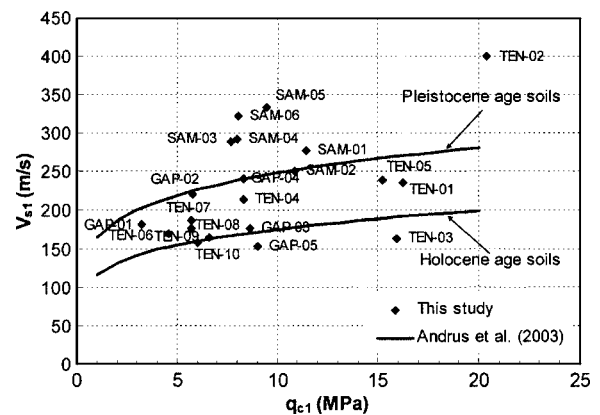


**Fig. 8.** Correlation between CPT  $q_{c1}$  values and shear wave velocity  $V_{s1}$  values



**Table 2.** Aging Correction Applied to Penetration Resistance and Shear Wave Velocity Data

| Site     | Location | $t$<br>(years)     | Mesri et al. (1990)<br>method   |                  |                       |                       |                  |                  |                       |                       |                   |                  |                       |                       |
|----------|----------|--------------------|---------------------------------|------------------|-----------------------|-----------------------|------------------|------------------|-----------------------|-----------------------|-------------------|------------------|-----------------------|-----------------------|
|          |          |                    | Kulhawy and Mayne (1990) method |                  |                       |                       | $\Delta e_R=5\%$ |                  |                       |                       | $\Delta e_R=10\%$ |                  |                       |                       |
|          |          |                    | $c_{aging}$                     | $[(N_1)_{60}]_R$ | $(q_{c1})_R$<br>(MPa) | $(V_{s1})_R$<br>(m/s) | $c_{aging}$      | $[(N_1)_{60}]_R$ | $(q_{c1})_R$<br>(MPa) | $(V_{s1})_R$<br>(m/s) | $c_{aging}$       | $[(N_1)_{60}]_R$ | $(q_{c1})_R$<br>(MPa) | $(V_{s1})_R$<br>(m/s) |
| Gapway   | GAP-01   | 450,000            | 1.38                            | 7                | 2.3                   | 171                   | —                | —                | —                     | —                     | —                 | —                | —                     | —                     |
|          | GAP-02   | 3,548              | 1.28                            | 9                | 4.3                   | 211                   | 3.24             | 3                | 1.7                   | 179                   | 4                 | 2                | 1.2                   | 169                   |
|          | GAP-03   | 5,038              | 1.29                            | 9                | 6.4                   | 169                   | 3.36             | 3                | 2.5                   | 143                   | 5                 | 2                | 1.8                   | 134                   |
|          | GAP-04   | 5,038 <sup>a</sup> | 1.29                            | 6                | 6.1                   | 230                   | 3.36             | 2                | 2.4                   | 193                   | 5                 | 2                | 1.7                   | 182                   |
|          | GAP-05   | 450,000            | 1.38                            | 12               | 6.3                   | 145                   | —                | —                | —                     | —                     | —                 | —                | —                     | —                     |
| Sampit   | SAM-01   | 450,000            | 1.38                            | 10               | 7.9                   | 261                   | —                | —                | —                     | —                     | —                 | —                | —                     | —                     |
|          | SAM-02   | 546                | 1.24                            | 11               | 8.4                   | 241                   | 2.63             | 5                | 3.9                   | 210                   | 3                 | 4                | 3.0                   | 201                   |
|          | SAM-03   | 450,000            | 1.38                            | 10               | 5.3                   | 272                   | —                | —                | —                     | —                     | —                 | —                | —                     | —                     |
|          | SAM-04   | 1,021              | 1.25                            | 11               | 6.1                   | 280                   | 2.82             | 5                | 2.7                   | 242                   | 4                 | 4                | 2.0                   | 230                   |
|          | SAM-05   | 1,648              | 1.26                            | 13               | 7.2                   | 321                   | 2.97             | 5                | 3.0                   | 275                   | 4                 | 4                | 2.3                   | 261                   |
|          | SAM-06   | 450,000            | 1.38                            | 7                | 5.6                   | 303                   | —                | —                | —                     | —                     | —                 | —                | —                     | —                     |
| Ten Mile | TEN-01   | 3,548              | 1.28                            | 14               | 12.2                  | 225                   | 3.24             | 6                | 4.8                   | 191                   | 4                 | 4                | 3.5                   | 180                   |
|          | TEN-02   | 3,548              | 1.28                            | 23               | 15.3                  | 383                   | 3.24             | 9                | 6.0                   | 325                   | 4                 | 7                | 4.4                   | 307                   |
| Hill A   | TEN-03   | 3,548              | 1.28                            | 13               | 11.9                  | 156                   | 3.24             | 5                | 4.7                   | 132                   | 4                 | 4                | 3.4                   | 125                   |
|          | TEN-04   | 3,548              | 1.28                            | 14               | 6.2                   | 205                   | 3.24             | 6                | 2.5                   | 174                   | 4                 | 4                | 1.8                   | 164                   |
|          | TEN-05   | 3,548              | 1.28                            | —                | 11.4                  | 229                   | 3.24             | —                | 4.5                   | 194                   | 4                 | —                | 3.3                   | 183                   |
| Ten Mile | TEN-06   | 200,000            | 1.37                            | 7                | 3.2                   | 161                   | —                | —                | —                     | —                     | —                 | —                | —                     | —                     |
|          | TEN-07   | 200,000            | 1.37                            | 4                | 4.0                   | 177                   | —                | —                | —                     | —                     | —                 | —                | —                     | —                     |
| Hill B   | TEN-08   | 200,000            | 1.37                            | 6                | 4.0                   | 167                   | —                | —                | —                     | —                     | —                 | —                | —                     | —                     |
|          | TEN-09   | 200,000            | 1.37                            | 4                | 4.2                   | 149                   | —                | —                | —                     | —                     | —                 | —                | —                     | —                     |
|          | TEN-10   | 200,000            | 1.37                            | 4                | 4.6                   | 156                   | —                | —                | —                     | —                     | —                 | —                | —                     | —                     |

<sup>a</sup>The sand boil at GAP-04 was not associated with a prehistoric earthquake therefore its age is based on the age of the adjacent sand boil at GAP-03.

and Gapway sites with sand deposits of 450,000 years in age. Talwani and Schaeffer (2001) found the paleoliquefaction features in freshly cut drainage ditches and used radiocarbon ages of dateable organic material that was trapped within the sand boil to associate the paleoliquefaction features with seven prehistoric earthquakes. Hu et al. (2002a) analyzed the SPT, CPT, and  $V_s$  data at these sites to determine the soil profile, identify the source sands, and determine their engineering properties. The results are summarized in Table 1. A graphical illustration of the CPT versus the  $V_s$  data at these sites is shown in Fig. 8 where they are compared to the correlation Eq. (15) proposed by Andrus et al. (2003). The correlation agrees well with the data used in this study for all the sites except Sampit.

In situ tests at the Sampit site were performed along a northwest-southeast-trending drainage ditch approximately 500 m in length (SAM-01 to SAM-06). SAM-02 and SAM-05 were in the vicinity of two small sand boils, and SAM-04 was in the vicinity of four large sand boils. Paleoliquefaction features found in SAM-02, SAM-04 and SAM-05 were associated with earthquakes that occurred 546, 1,021, and 1,648 years ago (Talwani and Schaeffer 2001). At the Gapway site, CPT and shear-wave velocity tests were conducted at five locations (GAP-01 to GAP-05). SPT tests were carried out at each location except GAP-04. Paleoliquefaction features found in GAP-02 and GAP-03 were associated with earthquakes that occurred 3,548 and 5,038 years ago (Talwani and Schaeffer 2001). The sand boil discovered at GAP-04 was not associated with a prehistoric earthquake therefore it is assumed that it was formed during the same earthquake as the nearby sand boil at location GAP-03, that is 5,038 years ago.

Paleoliquefaction features at the Ten Mile Hill Site associated with an earthquake that occurred 3,548 years ago (Talwani and Schaeffer 2001) were discovered in a drainage ditch. Geotechnical tests were carried out about 50 m to the southeast of the paleoliquefaction site (Ten Mile Hill site A) because of the heavy vegetation in this location. CPT and shear wave velocity tests were conducted at five locations (TEN-01 to TEN-05). SPT tests were carried out at each location except TEN-05. No sand boils

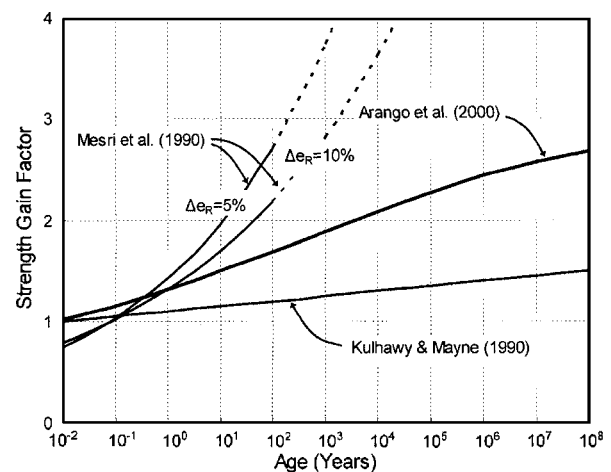


**Fig. 9.** Comparison of the correction factors for aging proposed by (a) Kulhawy and Mayne (1990); (b) Mesri et al. (1990); and (c) Arango et al. (2000)

**Table 3.** Cyclic Resistance Ratios (CRRs) for Freshly Deposited and Current (Aged) State of Soil

| Site            | Location | <i>t</i><br>(years) | <i>c</i> <sub>CRR</sub> | CRR for freshly<br>deposited state of soil |               |                                 | CRR for current<br>(aged) state of soil |               |                                 |
|-----------------|----------|---------------------|-------------------------|--|---------------|---------------------------------|---|---------------|---------------------------------|
|                 |          |                     |                         | SPT-<br>based                              | CPT-<br>based | <i>V<sub>s</sub></i> -<br>based | SPT-<br>based                           | CPT-<br>based | <i>V<sub>s</sub></i> -<br>based |
| Gapway          | GAP-01   | 450,000             | 2.38                    | 0.080                                      | 0.070         | 0.115                           | 0.190                                   | 0.166         | 0.275                           |
|                 | GAP-02   | 3,548               | 1.98                    | 0.101                                      | 0.087         | 1.216                           | 0.200                                   | 0.173         | —                               |
|                 | GAP-03   | 5,038               | 2.01                    | 0.095                                      | 0.108         | 0.112                           | 0.190                                   | 0.218         | 0.225                           |
|                 | GAP-04   | 5,038 <sup>a</sup>  | 2.01                    | 0.074                                      | 0.105         | —                               | 0.149                                   | 0.211         | —                               |
|                 | GAP-05   | 450,000             | 2.38                    | 0.130                                      | 0.107         | 0.074                           | 0.310                                   | 0.255         | 0.176                           |
| Sampit          | SAM-01   | 450,000             | 2.38                    | 0.109                                      | 0.134         | —                               | 0.258                                   | 0.319         | —                               |
|                 | SAM-02   | 546                 | 1.85                    | 0.123                                      | 0.143         | —                               | 0.227                                   | 0.264         | —                               |
|                 | SAM-03   | 450,000             | 2.38                    | 0.119                                      | 0.097         | —                               | 0.284                                   | 0.230         | —                               |
|                 | SAM-04   | 1,021               | 1.89                    | 0.121                                      | 0.104         | —                               | 0.229                                   | 0.197         | —                               |
|                 | SAM-05   | 1,648               | 1.92                    | 0.137                                      | 0.119         | —                               | 0.264                                   | 0.229         | —                               |
|                 | SAM-06   | 450,000             | 2.38                    | 0.080                                      | 0.099         | —                               | 0.190                                   | 0.235         | —                               |
| Ten Mile Hill A | TEN-01   | 3,548               | 1.98                    | 0.155                                      | 0.272         | —                               | 0.308                                   | 0.539         | —                               |
|                 | TEN-02   | 3,548               | 1.98                    | 0.260                                      | 0.458         | 0.293                           | 0.514                                   | 0.906         | —                               |
|                 | TEN-03   | 3,548               | 1.98                    | 0.144                                      | 0.260         | 0.088                           | 0.285                                   | 0.515         | 0.174                           |
|                 | TEN-04   | 3,548               | 1.98                    | 0.152                                      | 0.106         | 0.356                           | 0.302                                   | 0.209         | 0.704                           |
|                 | TEN-05   | 3,548               | 1.98                    | —  | 0.239         | —                               | —                                       | 0.472         | —                               |
| Ten Mile Hill B | TEN-06   | 200,000             | 2.28                    | 0.080                                      | 0.078         | 0.096                           | 0.182                                   | 0.177         | 0.218                           |
|                 | TEN-07   | 200,000             | 2.28                    | 0.060                                      | 0.085         | 0.129                           | 0.136                                   | 0.193         | 0.295                           |
|                 | TEN-08   | 200,000             | 2.28                    | 0.072                                      | 0.085         | 0.108                           | 0.164                                   | 0.194         | 0.245                           |
|                 | TEN-09   | 200,000             | 2.28                    | 0.060                                      | 0.088         | 0.079                           | 0.136                                   | 0.201         | 0.180                           |
|                 | TEN-10   | 200,000             | 2.28                    | 0.060                                      | 0.091         | 0.088                           | 0.136                                   | 0.206         | 0.201                           |

<sup>a</sup>The sand boil at GAP-04 was not associated with a prehistoric earthquake therefore its age is based on the age of the adjacent sand boil at GAP-03.

had been discovered in Ten Mile Hill Site B, even though widespread liquefaction was reported to have occurred in that location during the 1886 Charleston earthquake. SPT, CPT, and shear-wave velocity tests were conducted at five locations (TEN-06 to TEN-10).

The work presented herein considers that the in situ properties of the source sand at the location of a sand boil provide a liquefaction susceptibility index of a sand that liquefied as many years ago as the occurrence date of the prehistoric earthquake that is associated with it. Assuming that destruction of the preearthquake soil structure takes place during liquefaction (Olson et al. 2001) the age of the source sand at the sand boil locations is equal to the occurrence date of the associated earthquake. In addition, it is assumed that the in situ properties of the source sand at the locations where no sand boils were discovered provide a liquefaction susceptibility index of a sand deposit that never liquefied in the past therefore its age is equal to the geologic age of the deposit. At Ten Mile Hill site A the nearest paleoliquefaction feature was approximately 50 m to the northeast. Investigated locations were only 23–27 m apart from each other. Analysis of the in situ geotechnical data [see Hu et al. (2002a)] for all locations indicated that the soil profile does not significantly change within tens of meters. Thus it is believed that the soil properties encountered at the investigated locations are representative of those 50 m away at the location of the discovered sand boil. Consequently, the age of the source sand at all five locations in Ten Mile Hill site A is 3,548 years. At Ten Mile Hill site B where no sand boils were discovered the age of the source sand is equal to 200,000 years. The borings at Sampit were within about 10 m of the drainage ditch where the sand boils were discovered, and at Gapway they were within 2 m (Hu et al. 2002a). Thus it is believed that the

geotechnical test data in the vicinity of the sand boils are representative of those at the location of the sand boils. So, it is assumed that the age of the source sand at SAM-02, SAM-04, SAM-05, GAP-02, GAP-03, and GAP-04 is 546, 1,021, 1,648, 3,548, 5,038, and 5,038 years, respectively, and 450,000 years at the nonliquefied sites.

It is important to recognize that there is an inherent liquefaction resistance associated with fines content and its plasticity. For this study, the percentage of fines present at all investigated locations in the SCCP is small enough [ $0\% \leq FC \leq 9\%$ ;  $ave=4\%$  (Table 1)] for the source sands to be approximated as clean sands. The empirical relationships developed by Mesri et al. (1990); Kulhawy and Mayne (1990); and Arango et al. (2000) for clean sands are thus considered applicable to the old sand deposits encountered at all investigated locations in the SCCP. The only exception is indicated on the last segment of the Arango et al. (2000) correlation (see Fig. 5) which involves 30 million-years-old sand deposits (BSRI 1993, 1995) with a fines content ranging between 10 and 35%. This segment of the curve is not employed in the present work, however, as the soil deposits studied here do not exceed 450,000 years in age. In addition, the effect of the plasticity of the fines was neglected in the Arango et al. (2000) correlation and also in this work. This is reasonable because the plasticity associated with a small fines content is considered to be insufficient to exert a stronger effect on cyclic resistance than fines content alone (Koester 1994).

It is also important to consider the different effects of fines content in freshly deposited sands and aged sands. In freshly deposited sands, Andrianopoulos et al. (2001) reported that fines in small percentages decrease the void ratio of the soil without contributing to soil strength. Conversely, Salgado et al. (2000)

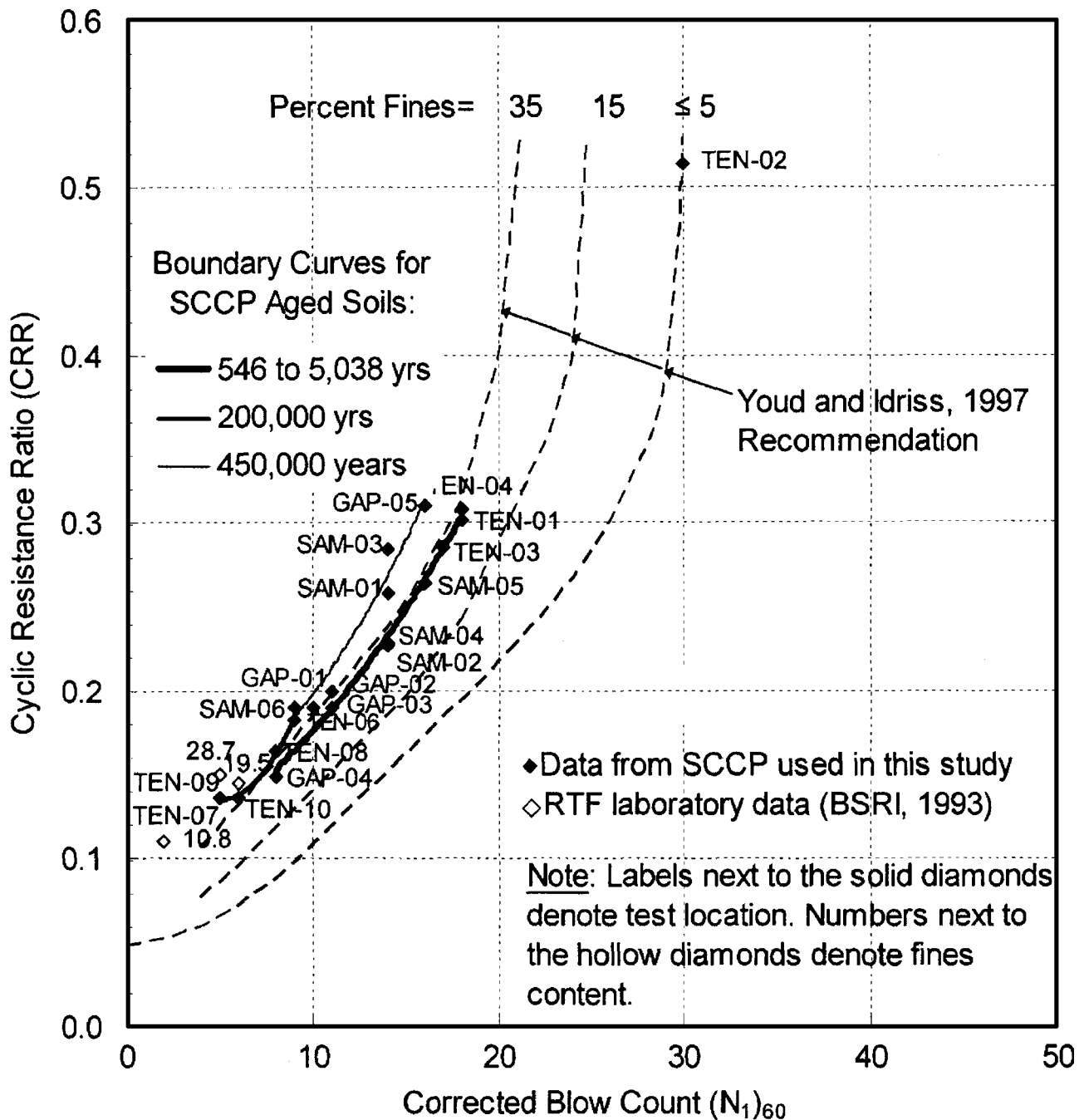


Fig. 10. Recommended boundary curves for the aged soil deposits in SCCP based on SPT blow count

showed that strength increases markedly with the addition of 5% and more nonplastic fines to sand, while stiffness decreases. In aged sands, it is possible that aging processes, such as the formation of precipitates or fabric evolution, may dominate the small fines content effect and cause a greater increase in the liquefaction resistance of the soil than the small fines content would. Additionally, it is possible that the presence of fines between sand particles affects the aging process itself and resulting behavioral response.

## Results

As a first step to utilize the proposed methodology, the in situ currently recorded penetration resistance and shear wave velocity

data from the four sites in the SCCP are corrected for aging using the Kulhawy and Mayne (1990) [Eq. (16)] and the Mesri et al. (1990) [Eq. (17)] method. For this work,  $t_R$ , in the Mesri et al. (1990) method, is selected equal to 30 days ( $=0.082$  years) and  $C_a/C_c$  equal to 0.02. Two values of  $\Delta e_R$ , 5 and 10%, are selected to represent a range of the change in relative density due to postliquefaction densification. For these values the corresponding  $C_D$  values are graphically determined from Fig. 4. In the same figure it is observed that  $C_D$  is also affected by the disturbance mechanism that induces liquefaction to the soil (e.g., blasting, vibrocompaction). In the absence of the earthquake as one of the disturbance mechanisms that induce liquefaction, the smaller values of  $C_D$  are hypothesized to be the most applicable for the case of an earthquake-induced liquefaction (G. Mesri, personal com-

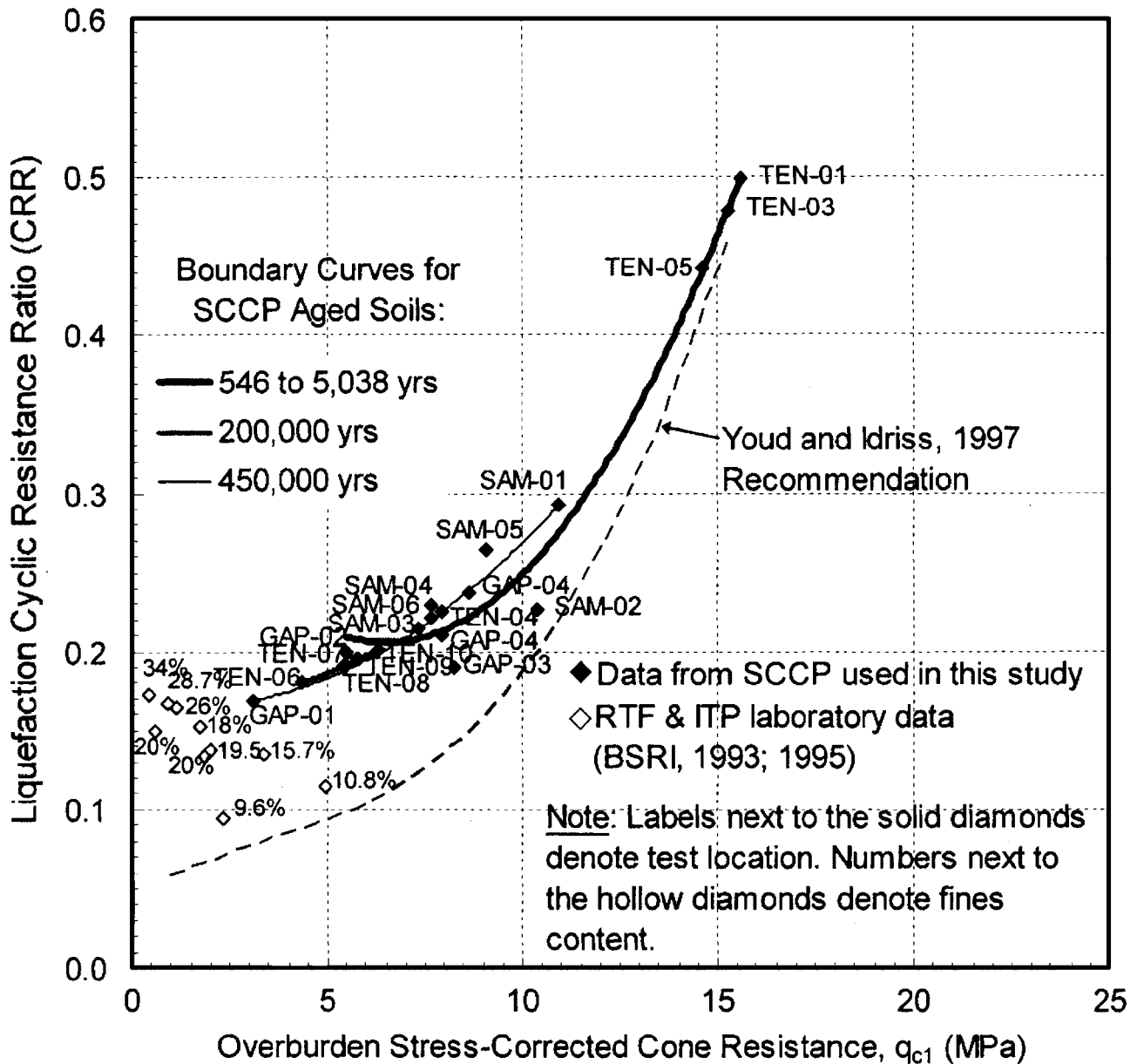


Fig. 11. CPT-based recommended boundary curve for the aged soil deposits in SCCP

munication, 2003). So, from Fig. 4 and the lower one from the two curves: for  $\Delta e_R=5\%$ ,  $C_D=5.5$ , and for  $\Delta e_R=10\%$ ,  $C_D=7.0$ . For locations that did not liquefy, the Mesri et al. (1990) method cannot be used since it is assumed that a disturbance mechanism as expressed by  $C_D$  never existed.

The corrected for aging in situ geotechnical data  $[(N_1)_{60}]_R$ ,  $(q_{c1})_R$ , and  $(q_{c1})_R$  which represent the soil at its freshly deposited state are presented for both methods in Table 2 (columns 5–7, 9–11, and 13–15). In the same table aging as described by the parameter  $t$  (column 3) as well as the corresponding correction factor  $c_{aging}$  as represented by  $c_A$  [Eq. (11)] for the Kulhawy and Mayne (1990) method and by the right hand side of Eq. (17) for the Mesri et al. (1990) method are also presented (columns 4, 8, and 12). A significant difference is observed between the estimated SPT, CPT, and  $V_s$  values of the soil at its freshly deposited state with the two different methods. The Mesri et al. (1990) method suggests the highest  $c_{aging}$  values thereby estimating the lowest SPT, CPT, and  $V_s$  values for the freshly deposited soil.

Fig. 9 illustrates how the aging correction factors for each method change with the age of the deposit. In the same figure, the correction factor for aging recommended by Arango et al. (2000) that applies to CRR is also illustrated and it appears to be for the most part lower than the correction factor for aging suggested by Mesri et al. (1990), which applies to CPT data. This observation contradicts the previous discussion about capturing of the aging by penetration resistance (SPT, CPT) and liquefaction resistance (CRR). The Mesri et al. (1990) method is based upon the results from the performance of ground modification techniques. Thus the basic limitation of this procedure is that disturbance is generated from a ground improvement technique and not from an earthquake event. Each event presumably produces a different ground motion resulting in a different subsurface liquefaction pattern. Thus densification (as expressed by  $\Delta e_r$ ) due to liquefaction from ground improvement can be significantly different than densification due to liquefaction from an earthquake.

Completion of the rest of this work (steps 2–4) will take into

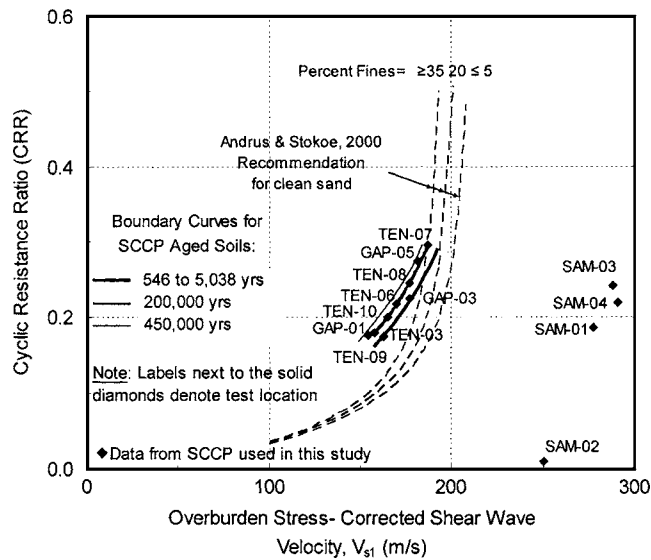


**Fig. 12.** Recommended boundary curves for the aged soil deposits in SCCP based on shear wave velocity

consideration only the results obtained from the Kulhawy and Mayne (1990) method where more confidence is shown. So, as a second step, the  $[(N_1)_{60}]_R$ ,  $(q_{c1})_R$ , and  $(V_{s1})_R$  values (columns 5, 6, and 7 in Table 2) for the soil at its freshly deposited state are employed to access the existing SPT-, CPT-, and  $V_s$ -based empirical relationships, respectively. The intersection points give the CRR values of the freshly deposited soil for the SPT-, CPT-, and

$V_s$ -based procedure. The results are presented in Table 3 (columns 5, 6, and 7). For locations such as TEN-01, TEN-02, TEN-05, SAM-01 to SAM-06, GAP-02, and GAP-04 the  $V_s$ -based CRR values cannot be obtained because the shear wave velocity there is higher than the upper limit of 215 m/s recommended by Andrus and Stokoe (2000). The approximation of the source sand with clean sand allows the empirical relationship proposed by Youd and Idriss (1997) for clean sands to be employed in the CPT-based procedure. For the other two procedures the fines content as given in Table 1 is used to interpolate between the curves.

CRR values for the aged sand deposits which represent the liquefaction resistance of the soil at its current state are calculated from Eq. (19) and presented in Table 3 (columns 8, 9, and 10). In the same table each location (column 2) along with the age of the source sand (column 3) and the corresponding strength gain factor  $c_{CRR}$  (column 4) are also presented.

Finally, the currently recorded penetration resistance and shear wave velocity data (columns 7, 8, and 9 in Table 1) are correlated with the calculated CRR values for old sand deposits encountered at the investigated locations in the SCCP. SPT-, CPT-, and  $V_s$ -based boundary curves are developed representative of the SCCP conditions and are compared with the existing empirical correlations for Holocene age soils in Figs. 10–12, respectively. The results for the old sand deposits are organized into three groups according to their age. No distinction for fines content is needed since the sands at these sites are considered to be nearly clean. As a result, three boundary curves for each in situ method are recommended for the SCCP, accounting for a fines content range between 0 and 9, and corresponding to sand deposits of 546–5,038, 200,000, and 450,000 years old.

**Table 4.** Estimated Peak Ground Accelerations Capable of Triggering Liquefaction Using Cyclic Stress Method for Earthquake Magnitude M7.5

| Site            | Location | Threshold peak ground acceleration (g) |           |              |   |           |              |
|-----------------|----------|--|-----------|--------------|---|-----------|--------------|
|                 |          | Accounting for soil aging (this study) |           |              | Not accounting for soil aging (Hu et al. 2002b) |           |              |
|                 |          | SPT-based                              | CPT-based | $V_s$ -based | SPT-based                                       | CPT-based | $V_s$ -based |
| Gapway          | GAP-01   | 0.31                                   | 0.26      | 0.43         | 0.17  | 0.13      | —            |
|                 | GAP-02   | 0.29                                   | 0.32      | —            | 0.19  | 0.15      | —            |
|                 | GAP-03   | 0.29                                   | 0.31      | 0.35         | 0.19  | 0.22      | —            |
|                 | GAP-04   | 0.24                                   | 0.31      | —            | 0.14  | 0.21      | —            |
|                 | GAP-05   | 0.48                                   | 0.33      | 0.27         | 0.27  | 0.23      | —            |
| Sampit          | SAM-01   | 0.33                                   | 0.31      | —            | 0.20  | 0.28      | —            |
|                 | SAM-02   | 0.24                                   | 0.25      | —            | 0.17  | 0.22      | —            |
|                 | SAM-03   | 0.31                                   | 0.23      | —            | 0.18  | 0.14      | —            |
|                 | SAM-04   | 0.25                                   | 0.22      | —            | 0.17  | 0.14      | —            |
|                 | SAM-05   | 0.26                                   | 0.22      | —            | 0.18  | 0.17      | —            |
|                 | SAM-06   | 0.20                                   | 0.22      | —            | 0.11  | 0.14      | —            |
| Ten Mile Hill A | TEN-01   | 0.41                                   | 0.61      | —            | 0.27  | —         | —            |
|                 | TEN-02   | 0.66                                   | —         | —            | 0.59  | —         | —            |
|                 | TEN-03   | 0.32                                   | 0.49      | 0.21         | 0.21  | 0.53      | —            |
|                 | TEN-04   | 0.34                                   | 0.23      | —            | 0.22  | 0.15      | —            |
|                 | TEN-05   | —                                      | 0.49      | —            | —   | 0.54      | —            |
| Ten Mile Hill B | TEN-06   | 0.23                                   | 0.23      | 0.30         | 0.12  | 0.11      | —            |
|                 | TEN-07   | 0.16                                   | 0.23      | 0.37         | 0.08  | 0.12      | —            |
|                 | TEN-08   | 0.19                                   | 0.23      | 0.31         | 0.11  | 0.12      | —            |
|                 | TEN-09   | 0.18                                   | 0.26      | 0.25         | 0.08  | 0.13      | —            |
|                 | TEN-10   | 0.17                                   | 0.25      | 0.26         | 0.09  | 0.13      | —            |

In Figs. 10 and 11, the newly developed boundary curves (SPT- and CPT-based, respectively) for the old sand deposits in the SCCP are compared to the ones recommended by Youd and Idriss (1997) for young soil deposits. The recommended boundary curves lay to the left of the existing curves indicating that the aged soil deposits in SCCP possess more resistance to liquefaction than would be specified by the currently existing correlations if aging were not considered. Note that a rigorous comparison between the newly developed (SCCP) and currently existing (California, China, and Japan) boundary curves requires consideration of the different geologic settings, in relation to the nature of soil particles, fabric, structure, and stress state.

To emphasize the trends observed in the boundary curves developed for aged soils, the data reported in BSRI (1993, 1995) which represent results from cyclic triaxial tests performed on undisturbed samples of sand obtained from two sites (RTF and ITP) in the location of the Savannah River Site (SRS) are shown (hollow diamonds) in Fig. 11. The same data but only for the RTF site are shown in Fig. 10. Numbers next to the hollow diamonds represent the fines content. The SRS data are in good agreement with the newly developed boundary curve for aged soils, being both to the left of the Youd and Idriss (1997) recommendation. However, it should be pointed out that the SRS data involve older sand deposits (30 million years) than the ones studied here (up to 450,000 years old). In addition the percentage of fines present in the SRS samples (10–35%) is significantly higher than the fines present in the samples used to develop the boundary curves for the SCCP.

In Fig. 12 the  $V_s$ -based boundary curves for the old sand deposits in SCCP are compared with the Andrus and Stokoe (2000) recommendation. Due to the relatively high shear wave velocities recorded at several of the investigated locations (TEN-01, TEN-02, TEN-04, TEN-05, SAM-05, SAM-06, GAP-02, and GAP-04) these points do not appear on the plot. This is especially true for the results for the Sampit site which do not correlate well with those from the other paleoliquefaction sites. This discrepancy is an extension of the discrepancy observed in Fig. 8 and is attributed to the high shear wave velocities currently recorded in all Sampit locations.

Using the new boundary curves for aged soils developed for an earthquake magnitude M7.5, and the cyclic stress method [Eq. (1)] the current threshold acceleration required to trigger liquefaction at each one of the four investigated sites is calculated based on the currently recorded SPT, CPT, and  $V_s$  data. The estimated acceleration levels are listed in Table 4 where they are compared with the ones obtained by Hu et al. (2002b) for the same sites using the same data but not accounting for soil aging. Accounting for soil aging in the cyclic stress method yields higher values of the peak ground acceleration required to trigger liquefaction than when aging is not taken into account. The results indicate that accounting for soil aging at Ten Mile Hill sites A and B, Sampit, and Gapway increases the minimum acceleration required currently to cause liquefaction by a factor of 1.3, 2, 1.5, and 1.7, respectively (average for all the locations at a site). On the average for all the sites the estimated acceleration in this study and the one by Hu et al. (2002b) differ by a factor of 1.6 suggesting that the sand deposits in the SCCP are 60% more resistant to liquefaction induced by an earthquake M7.5 than indicated by the existing liquefaction resistance empirical correlations for young soil deposits.

## Summary and Conclusions

Soil aging has an effect on the liquefaction resistance of a sand deposit. Therefore it was the objective of this work to account for the age of the soil deposit when evaluating the liquefaction potential. The methodology that was developed incorporated soil aging into the parameters involved in the currently available boundary curves for assessing liquefaction potential, valid only for Holocene age soils. The involved parameters are the penetration resistance or shear wave velocity of the soil and the cyclic resistance ratio. Correction factors that comprise the effect of time were applied to both parameters. The final result is a relationship between the currently recorded in situ indices (SPT, CPT, and  $V_s$ ) and aged CRR values, yielding new empirical boundary curves for aged soils. Geotechnical data from four paleoliquefaction sites in the SCCP were used to illustrate the methodology. The newly developed boundary curves that describe the liquefaction potential of old sand deposits at the specific sites in the SCCP were compared to the ones previously developed for Holocene age deposits. The findings are as follows.

- Accounting for aging of the old sand deposits in the SCCP yields less conservative results regarding the liquefaction resistance than when not accounting for aging. The modified boundary curves are shifted to the left of the currently existing curves for Holocene age soils indicating that old soil deposits are more resistant to liquefaction than if aging were not considered.
- Minimum peak ground acceleration required to cause liquefaction of the old sand deposits in the SCCP was estimated to differ by a factor of 1.6 from the case where soil aging is not taken into consideration. Thus it is suggested that the liquefaction resistance of the old sand deposits in the SCCP is 60% higher than indicated by the existing liquefaction resistance empirical correlations for young soil deposits.

## Acknowledgments

The writers wish to thank Bechtel Savannah River Company for providing the CPT and shear wave velocity data. The SPT data were collected with funding provided by the Nuclear Regulatory Commission. Deep appreciation is extended by the first writer to her former employer Panagiotis Vettas of OTM, Inc., Greece, for his support during the course of this study.

## References

- Andrianopoulos, I. K., Bouckovalas, G. D., and Papadimitriou, A. G. (2001). "A critical state evaluation of fines effect on liquefaction potential." *Proc., 4th Int. Conf. on Recent Advances in Geotechnical Earthquake Engineering and Soil Dynamics and Symposium in Honor of Professor W. D. Liam Finn*, University of Missouri-Rolla, CD-ROM, San Diego.
- Andrus, R. D., Piratheepan, P., and Juang, C. H. (2003). "Shear wave velocity–penetration resistance correlations for ground shaking and liquefaction hazards assessment." (<http://erp-web.er.usgs.gov/reports/annsum/vol43/pt/01g0007.pdf>) (Feb. 8, 2003).
- Andrus, R. D., and Stokoe, K. H., II (2000). "Liquefaction resistance of soils from shear-wave velocity." *J. Geotech. Geoenviron. Eng.*, 126(11), 1015–1025.
- Arango, I., Lewis, M. R., and Kramer, C. (2000). "Updated liquefaction potential analysis eliminates foundation retrofitting of two critical structures." *Soil Dyn. Earthquake Eng.*, 20, 17–25.

- Arango, I., and Miguez, R. E. (1996). "Investigation of the seismic liquefaction of old sand deposits." *Rep. on Research, Bechtel Corporation, National Science Foundation Grant No. CMS-94-16169*, San Francisco.
- Bechtel Savannah River, Inc. (BSRI). (1993). "Savannah River Site Replacement Tritium Facility (233H) geotechnical investigation (U)." *WSRC-RP-93-606*, Vol. 3.
- Bechtel Savannah River, Inc. (BSRI). (1995). "In tank precipitation facility (ITP) and H-Tank Farm (HTF) geotechnical report (U)." *WSRC-TR-95-0057*, Rev. 0, Vol. 6.
- Dowding, C. H., and Hryciw, R. D. (1986). "A laboratory study of blast densification of saturated sand." *J. Geotech. Eng.*, 112(2), 187-199.
- Ellis, C., and De Alba, P. (1999). "Acceleration distribution and epicentral location of the 1755 Cape Ann earthquake from case histories of ground failure." *Seismol. Res. Lett.*, 70(6), 758-773.
- Hu, K., Gassman, S. L., and Talwani, P. (2002a). "In-situ properties of soils at paleoliquefaction sites in the South Carolina Coastal Plain." *Seismol. Res. Lett.*, 73(6), 964-978.
- Hu, K., Gassman, S. L., and Talwani, P. (2002b). "Magnitudes of prehistoric earthquakes in the South Carolina Coastal Plain from geotechnical data." *Seismol. Res. Lett.*, 73(6), 979-991.
- Joshi, R. C., Achari, G., Kaniraj, S. R., and Wijeweera, H. (1995). "Effect of aging on the penetration resistance of sands." *Can. Geotech. J.*, 32(5), 767-782.
- Koester, J. P. (1994). "The influence of fines type and content on cyclic strength." *Conf. Proc., Ground Failures under Seismic Conditions, Geotechnical Special Publication No. 44*, S. Prakash, ed., 17-33.
- Kramer, C., and Arango, I. (1998). "Aging effects on the liquefaction resistance of sand deposits: A review and update." *Proc., Eleventh European Conf. on Earthquake Engineering*, A.A. Balkema, CD-ROM, Bisch, Philippe, Pierre Labbe, and Alain Pecker, eds., Paris, Abstract Vol. 184.
- Kulhawy, F. H., and Mayne, P. W. (1990). "Manual on estimating soil properties for foundation design." *Final Rep. 1493-6, EL-6800*, Electric Power Research Institute, Palo Alto, Calif.
- Lewis, M. R., Arango, I., Kimball, J. K., and Ross, T. E. (1999). "Liquefaction resistance of old sand deposits." *Proc., 11th Panamerican Conf. on Soil Mechanics and Geotechnical Engineering*, Foz do Iguassu, Brasil, 821-829.
- Mesri, G., Feng, T. W., and Benak, J. M. (1990). "Postdensification penetration resistance of clean sands." *J. Geotech. Eng.*, 116(7), 1095-1115.
- Mitchell, J. K. (1986). "Practical problems from surprising soil behavior." *J. Geotech. Eng.*, 112(3), 259-289.
- Mitchell, J. K., and Solymar, Z. V. (1984). "Time-dependent strength gain in freshly deposited or densified sand." *J. Geotech. Eng.*, 110(11), 1559-1576.
- Olson, S. M., Obermeier, S. F., and Stark, T. D. (2001). "Interpretation of penetration resistance for back-analysis at sites of previous liquefaction." *Seismol. Res. Lett.*, 72(1), 46-59.
- Salgado, R., Bandini, P., and Karim, A. (2000). "Shear strength and stiffness of silty sand." *J. Geotech. Geoenviron. Eng.*, 126(5), 451-462.
- Schmertmann, J. H. (1987). "Discussion of 'Time-dependent strength gain in freshly deposited or densified sand,' by James K. Mitchell and Zoltan V. Solymar." *J. Geotech. Eng.*, 113(2), 173-175.
- Schmertmann, J. H. (1991). "The mechanical aging of soils." *J. Geotech. Eng.*, 117(9), 1288-1330.
- Seed, H. B. (1979). "Soil liquefaction and cyclic mobility evaluation for level ground during earthquakes." *J. Geotech. Eng. Div., Am. Soc. Civ. Eng.*, 105(2), 201-255.
- Seed, H. B., and Idriss, I. M. (1971). "Simplified procedure for evaluating soil liquefaction potential." *J. Soil Mech. Found. Div.*, 97(9), 1249-1273.
- Seed, H. B., Idriss, I. M., and Arango, I. (1983). "Evaluation of liquefaction potential using field performance data." *J. Geotech. Eng.*, 109(3), 458-482.
- Seed, H. B., Tokimatsu, K., Harder, L. F., and Chung, R. M. (1984). "The influence of SPT procedures on soil liquefaction resistance evaluations." *Earthquake Engineering Research Center, Rep. No. UCB/EERC 84/15*, Univ. of California, Berkeley, Calif.
- Seed, H. B., Tokimatsu, K., Harder, L. F., and Chung, R. M. (1985). "The influence of SPT procedures in soil liquefaction resistance evaluations." *J. Geotech. Eng.*, 111(12), 1425-1445.
- Skempton, A. W. (1986). "Standard penetration test procedures and the effects in sands of overburden pressure, relative density, particle size, aging, and overconsolidation." *Geotechnique*, 36(3), 425-447.
- Stark, D., Obermeier, S. F., Newman, E. J., and Stark, J. M. (2002). "Interpretation of ground shaking from paleoliquefaction features." (<http://erp-web.er.usgs.gov/reports/annsum/vol43/cu/g0030.pdf>) (Feb. 8, 2003).
- Talwani, P., and Schaeffer, W. T. (2001). "Recurrence rates of large earthquakes in the South Carolina Coastal Plain based on paleoliquefaction data." *J. Geophys. Res.*, 106(B4), 6621-6642.
- Youd, T. L., and Hoose, S. N. (1977). "Liquefaction susceptibility and geologic setting." *Proc., 6th World Conf. on Earthquake Engineering*, New Delhi, India, Vol. 6, 37-42.
- Youd, T. L., and Idriss, I. M. (1997). "Summary report," *Proc., NCEER Workshop on Evaluation of Liquefaction Resistance of Soils, Tech. Rep. NCEER-97-0022*, T. L. Youd and I. M. Idriss, eds., National Center for Earthquake Engineering Research, Buffalo, 1-40.
- Youd, T. L., and Perkins, D. M. (1978). "Mapping liquefaction-induced ground failure potential." *J. Geotech. Eng. Div., Am. Soc. Civ. Eng.*, 104, 433-446.